Research Paper
Computational Methods for Differential Equations
http://cmde.tabrizu.ac.ir
Vol. 12, No. 3, 2024, pp. 523-543
DOI:10.22034/cmde.2023.57934.2435

A mathematical study on the non-linear boundary value problem of a porous fin

V. Ananthaswamy[1,*], R. R. Subanya[2], and S. Sivasankari[2]
[1]Research Centre and PG Department of Mathematics,The Madura College, Madurai, Tamil Nadu, India.
[2]Research Scholar, Research Centre and PG Department of Mathematics, The Madura College, Madurai, Tamil Nadu, India.

Abstract

An analytical study of two different models of rectangular porous fins are investigated using a new approximate analytical method, the Ananthaswamy-Sivasankari method. The obtained results are compared with the numerical solution, which results in a very good agreement. The impacts of several physical parameters involved in the problem are interlined graphically. Fin efficiency and the heat transfer rate are also calculated and displayed. The result obtained by this method is in the most explicit and simple form. The convergence of the solution determined is more accurate as compared to various analytical and numerical methods.

Keywords. Longitudinal fin, Darcy's model, Insulated tip, Ananthaswamy-Sivasankari method (ASM), Magneto hydrodynamics (MHD)..
2010 Mathematics Subject Classification. 34B15; 34B60; 34E05; 34E10.

1. Introduction

Significant applications for increasing heat transfer concerning hot surfaces of different appliances can be found in industrial, technological, and engineering machinery, such as air conditioners, car radiators, computer equipment, CPUs, refrigerators, etc. The rate of heat transmission from the heated exterior to the nearby fluids is increased for this purpose by using the optimum extended surfaces. The choice of a certain fin type is influenced by the primary surface's geometry. The production, pricing, and ease of installation of the materials are often taken into account while determining a fin's profile. Finding the fin profile that offers the fastest heat transfer rate for a specific fin has been the focus of numerous researchers. The optimal shape of the fin, which can be circular, parabolic, or rectangular, has been described. Because of its simple construction and straightforward manufacture, the rectangular fin was most widely used.

Alkam and Al-Nimr [1] employed porous materials with significant thermal conductivity to enhance the thermal performance of various thermal systems. The influence of utilizing porous fins on the transmission of heat from a heated flat the surface was examined numerically by Kiwan and Al-Nimr [20]. Heat transmission via a porous fin situated on a vertical surface was numerically addressed by Kiwan [22] adopting laminar natural convection as well as MHD impact of laminar mixed convection was studied by Taklifi et al. [40]. Furthermore, Kiwan and Zeitoun [21] studied the impact of employing porous fins in the annulus of two focused cylinders numerically. Comparing the application of porous fins to traditional solid fins, they discovered that the latter increased the heat transfer coefficient by almost 70%.

Modern engineering, applied mathematics, physics, and newer disciplines of research, particularly heat transfer difficulties, all rely extensively on fin issues and phenomena. Many approximation analytical strategies have been utilized to tackle these kinds of problems, including the HAM (Khani et al. [19]), Least Square Method, and DTM (Aziz and Bouaziz [3]; Hatami et al. [16]). Oguntala et al. [27–31] used a variety of methods to tackle fin problems, including the Daftardar-Gejiji and Jarari method (DJM) [31], the Haar wavelet collocation technique [29], the Chebyshev collocation spectral approaches [30], and the Homotopy perturbation method [27]. In a naturally convective porous

Received: 10 August 2023 ; Accepted: 21 November 2023.
∗ Corresponding author. Email: ananthu9777@gmail.com.

fin exposed to some specified temperature, Das et al. [6, 7] tested unidentified and conceivable mixtures of variables. He calculated multiple fin characteristics in order to solve an inverse problem using simulated annealing.

Recently, research on porous fin performance with optimal design assessment has been a fascinating topic. Amirkolaei et al. [2] analyzed the MHD of a permeable fin attached to a vertically isothermal surface exhibiting temperature-dependent internal heat generation with the help of HAM. In Balram Kundu et al. [4], a detailed analytical estimate regarding porous fin performance and optimal design evaluation was presented. Dipankar Bhanja et al. [8] thermally analyzed the porous pin fin utilized in electronic cooling via ADM. Ganji et al. [9] applied two methods (VIM and PM) to resolve the temperature gradient of a porous fin. Ghasemi et al. [11] examined two different cases of convective fin using the DTM (Differential transformation method). Also, he investigated both solid as well porous fins [10] via DTM. Hatami et al. [14] evaluated heat transmission equations with entirely soaked hemispherical permeable fins via the least squares technique (LSM [15, 17]), and they obtained the most exact analytical solution for them. Also, he studied and reported that for fin shapes: convex, rectangular, exponential, and triangular, the rate related to heat transfer varied from maximum to minimum values, respectively [13]. Nowadays, numerous solution types include periodic, breather, and soliton solutions for these types of non-linear issues and wave systems [24, 25].

Although fin inclination is crucial regarding the porous fin, numerous authors describe into how it affects thermal performance. Gireesha et al. [12] have shown the impacts of radiation and also natural convection on a longitudinal porous fin connected to an inclined surface using Darcy's model via DTM. In several other studies, Sobamowo et al.[37–39], Gireesha and Sowmya [12], Jasim et al. [18], and Oguntala et al. [28] examined the consequences of fin inclination on the thermal performance associated with elongated surfaces. Singh et al. [23] examined the thermal evaluation of a porous stepped fin constructed with several porous ceramic components. The dynamic behavior of fins having various forms and varying thermal characteristics, including the internal generation of heat, was explored by Mosayebidorcheh et al. [26].

Due to the majority of the works using numerical approaches, we were compelled by the aforementioned studies to look into these kinds of porous fin challenges via analytical techniques. In this study, we looked at two models of rectangular fins. For these two models, we apply ASM to achieve an approximate analytical solution. A good agreement is seen when the outcomes are compared to the numerical solution. The fin efficiency as well as the heat transfer rate are computed and graphically depicted.

2. Mathematical description of the problem

Here we have considered two mathematical models. One is a rectangular fin having a constant magnetic field, while the other is a convective-radiative longitudinal porous fin inclined at some angle. The brief constructions for the mentioned models are mathematically described and given below.

2.1. Rectangular porous fin having a unique magnetic field in such a vertical isothermal surface-radiate heat transfer, a finite-length fin with an insulated tip, and Darcy's model to realistically simulate the flow through porous media [32].

. Here, a rectangular porous fin Figure 1 with uniform cross-sectional area A, length L, width W, and thickness t is taken into consideration under the following assumptions:

•The fin is constructed of a porous material that enables a flow to pass through it.

•The single-phase fluid has saturated the porous medium, which is homogeneous and isotropic.

•When a magnetic field is uniform and is supplied in the y-axis direction, the temperature within the fin is only a term which contains x.

•Darcy's form is employed to analyze the velocity of the flow within a porous medium exhibiting negligible influence of the induced and imposed magnetic field together with the induced electrical field owing to the polarization effect.

The one-dimensional energy balance equation for the slice segment of the fin thickness Δx under steady-state

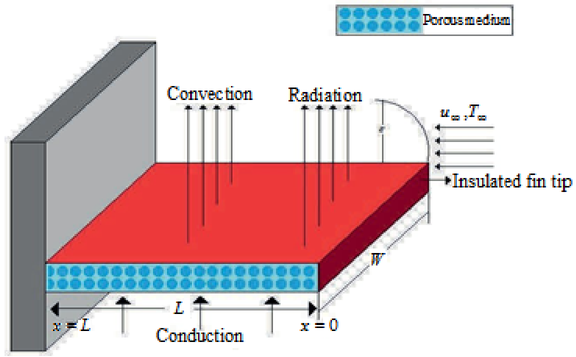

FIGURE 1. The geometry of a rectangular fin configuration.

conditions is provided by [19, 40],

$$q(x) - q(x + \Delta x) = m\, c_p\, (T(x) - T(\infty)) + hP(1-\epsilon)\,(T(x) - T(\infty)) + \frac{(J_C \times J_C)}{\sigma} + P\,\Delta x\, \sigma_{st}\, \bar{\epsilon} \left(T(x)^4 - \frac{y}{\epsilon} T(\infty)^4\right), \tag{2.1}$$

where J_C is the conduction current intensity, and it is described by

$$J_C = \sigma\,(V \times B + E)\,, \tag{2.2}$$

and, J is the total current intensity specified by

$$J = J_C + \rho\, \bar{\epsilon}\, V. \tag{2.3}$$

The fluid's mass flow rate $\bar{m}$ via a porous medium is expressed as

$$\bar{m} = \rho\, w\, \bar{v_w}\, \Delta. \tag{2.4}$$

When the flow along an impermeable medium is taken into account along with the passage velocity $\bar{v_w}$, the results of Darcy's model is as follows:

$$\bar{v_w} = \frac{k\, \beta\, g\, (T(x) - T(\infty))}{v}. \tag{2.5}$$

At the fin's base, conduction and radiation have the following relationship:

$$q_{fin\, base} = q_{radiation} + q_{conduction}. \tag{2.6}$$

The Rosseland diffusion estimates [33] are defined by Fourier's law of conduction and the radiation heat flux term as follows:

$$q_{conduction} = k_{eff}\, A_b \frac{dT}{dx},\;\; q_{radiation} = \frac{4\sigma_{st}}{3\beta_r} \frac{dT^4}{dx}. \tag{2.7}$$

If Eqs. (2.2)-(2.7) are substituted for Eq. (2.1), it results in

$$\frac{d}{dx}\left[\frac{dT}{dx} + \frac{4\sigma}{3\beta_r\, k_{eff}} \frac{dT^4}{dx}\right] = \frac{\rho\, c_p\, g\, k\, \beta}{b\, v\, k_{eff}} (T(x) - T(\infty))^2 + \frac{h\, P\, (1-\epsilon)}{k_{eff}} (T(x) - T(\infty)) + \frac{(J_C \times J_C)}{\sigma\, k_{eff}\, A_b} + \frac{P\, \sigma_{st}\, \bar{\epsilon}}{k_{eff}\, A_b} \left(T(x)^4 - T(\infty)^4\right). \tag{2.8}$$

The electromagnetic force in Eq. (2.1) assumes its form $\frac{(J_C \times J_C)}{\sigma} = \sigma\, B_0^2\, u^2$ when the magnetic field and the induced current are neglected.

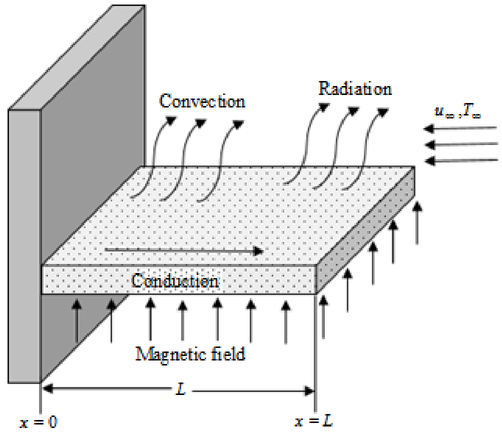

FIGURE 2. Schematic configuration of the convective-radiative longitudinal porous fin subjected to a magnetic field.

By employing the dimensionless parameters

$$\theta = \frac{T(x) - T_\infty}{T_b - T_\infty},\ \zeta = \frac{x}{L},\ \theta_b = \frac{T_b}{T_\infty},\ R_a = \frac{g\,k\,\beta\,b\,(T_b - T_\infty)}{y\,v\,k_r},\ N_c = \frac{P\,b\,h}{k_{eff}\,A},$$
$$N_r = \frac{4\,\sigma_{st}\,L\,T_\infty^3}{k_{eff}},\ H = \frac{\sigma\,B_0^2\,u^2}{k_0\,A},\ R_d = \frac{4\,\sigma_{st}\,T_\infty^3}{3\,\beta_r\,k_{eff}}. \tag{2.9}$$

Eq. (2.8) yields

$$\frac{d^2\theta}{d\zeta^2} - \frac{R_a}{(1 + 4\,R_d)}\theta^2 - \frac{[N_c\,(1-\epsilon) + N_r + H]}{(1 + 4\,R_d)}\theta = 0, \tag{2.10}$$

with the boundary conditions

$$\left.\frac{d\theta}{d\zeta}\right|_{\zeta=1} = 0,\ \ and\ \ \theta\Big|_{\zeta=0} = 1, \tag{2.11}$$

where R_a stands for a modified Rayleigh number, N_c means a convection–conduction parameter, N_r is a surface-ambient radiation parameter, H refers to a Hartman parameter, R_d represents a Radiation–conduction parameter and ϵ is porosity. In this article, we considered and investigated a finite-length fin with only an insulated tip, where there is no heat transmission.

2.2. The combined effects of MHD in addition to fin surface tilting together on the thermal behavior of a convective-radiative porous fin exhibiting temperature-invariant thermal transmission [36].

. As seen in Figure 2, consider a longitudinal rectangular fin with pores capable of radiative and convective heat transmission. As depicted in Figure 3, the fin has an angle of inclination γ with respect to the horizontal axis (x-axis). The porous medium is considered to be homogeneous, isotropic, and saturated with single-phase fluid in order to establish the porous fin's thermal model. The fluid surface around the fin and its physical and thermal characteristics are fixed. According to Figure 2, the only place where the temperature changes in the fin is along its length and the fin base makes perfect contact with the primary surface.

The energy balance is determined by the assumptions and with the help of Darcy's model, as follows:

$$q_x - \left(q_x + \frac{\delta q}{\delta x}dx\right) = \dot{m}\,c_p\,(T - T_a) + h\,P\,(1-\epsilon)\,(T - T_a)\,dx + \sigma\,\epsilon\,P\,\left(T^4 - T_a^4\right)dx + \frac{(J_C \times J_C)}{\sigma}dx. \tag{2.12}$$

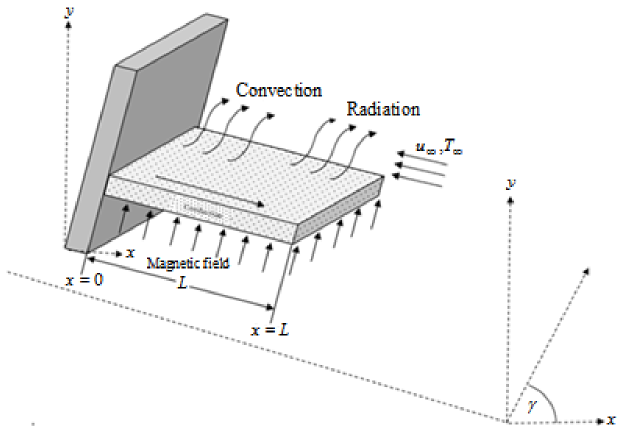

FIGURE 3. Schematic configuration of a convective-radiative longitudinal porous fin inclined at an angle γ to the horizontal axis.

The mass flow rate of the fluid through the pores is expressed as

$$\dot{m} = \rho\, u(x)\, W\, dx. \tag{2.13}$$

Moreover, the fluid velocity is specified as

$$u(x) = \frac{g\, K\, b_R\, (T - T_a)\ sin(\gamma)}{v}. \tag{2.14}$$

Then, Eq. (2.12) becomes

$$q_x - \left(q_x + \frac{\delta q}{\delta x} dx\right) = \frac{\rho\, c_p\, g\, K\, \beta_R}{v}\,(T - T_a)^2\ sin(\gamma)\, dx + h\, P\,(1-\epsilon)\,(T - T_a)\, dx$$
$$+ \sigma\, \epsilon\, P\,\left(T^4 - T_a^4\right) dx + \frac{(J_C \times J_C)}{\sigma} dx. \tag{2.15}$$

As $dx \to 0$, Eq. (2.15) reduces

$$-\frac{dq_x}{dx} = \frac{\rho\, c_p\, g\, K\, \beta_R}{v}\,(T - T_a)^2\ sin(\gamma) + h\, P\,(1-\epsilon)\,(T - T_a) + \sigma\, \epsilon\, P\,\left(T^4 - T_a^4\right) + \frac{(J_C \times J_C)}{\sigma}. \tag{2.16}$$

Applying Fourier's law to the solid's heat conduction, one must:

$$q_c = -k_{eff}\, A_{cr}\, \frac{dT}{dx}, \tag{2.17}$$

where the fin's effective thermal conductivity is stated as

$$k_{eff} = -\phi\, k_f + (1-\phi)\, k_s. \tag{2.18}$$

The radiative heat transmission rate can be expressed in the following way using the Rosseland Diffusion Approximation [33]:

$$q_R = -\frac{4\, \sigma\, A_{cr}}{3\, \beta_R}\frac{dT^4}{dx}. \tag{2.19}$$

From Eqs. (2.17) and (2.19), the total rate for heat transfer is obtained by

$$q_T = -k_{eff}\, A_{cr}\frac{dT}{dx} - \frac{4\, \sigma\, A_{cr}}{3\, \beta_R}\frac{dT^4}{dx}. \tag{2.20}$$

Substitution of Eq. (2.20) into Eq. (2.16) leads to

$$\frac{d}{dx}\left(k_{eff}\,A_{cr}\frac{dT}{dx}+\frac{4\,\sigma\,A_{cr}}{3\,\beta_R}\right)=\frac{\rho\,c_p\,g\,K\,\beta_R}{v}\left(T-T_a\right)^2\,sin(\gamma)+h\,P\,(1-\epsilon)\,(T-T_a)$$
$$+\sigma\,\epsilon\,P\,\left(T^4-T_a^4\right)+\frac{(J_C\times J_C)}{\sigma}. \tag{2.21}$$

The governing equation for the necessary heat transfer is provided by the expansion of the first term to Eq. (2.21).

$$\frac{d^2T}{dx^2}+\frac{4\,\sigma}{3\,k_{eff}\,\beta_R}\frac{d}{dx}\left(\frac{dT^4}{dx}\right)-\frac{\rho\,c_p\,g\,K\,\beta_R}{t\,v\,k_{eff}}\left(T-T_a\right)^2\,sin(\gamma)$$
$$-\frac{h\,P\,(1-\epsilon)\,(T-T_a)}{t\,k_{eff}}-\frac{\sigma\,\epsilon}{t\,k_{eff}}\left(T^4-T_a^4\right)-\frac{(J_C\times J_C)}{\sigma}=0. \tag{2.22}$$

The boundary conditions are:

$$x=0,\ \ \frac{dT}{dx}=0,$$
$$x=L,\ \ T=T_b. \tag{2.23}$$

But

$$\frac{(J_C\times J_C)}{\sigma}=\sigma\,B_0^2\,u^2. \tag{2.24}$$

After substituting Eq. (2.24) with Eq. (2.22), we have

$$\frac{d^2T}{dx^2}+\frac{4\,\sigma}{3\,k_{eff}\,\beta_R}\frac{d}{dx}\left(\frac{dT^4}{dx}\right)-\frac{\rho\,c_p\,g\,K\,\beta_R}{t\,v\,k_{eff}}\left(T-T_a\right)^2\,sin(\gamma)$$
$$-\frac{h\,P\,(1-\epsilon)\,(T-T_a)}{t\,k_{eff}}-\frac{\sigma\,\epsilon}{t\,k_{eff}}\left(T^4-T_a^4\right)-\frac{\sigma\,B_0^2\,u^2}{k_{eff}\,A_{cr}}\,(T-T_a)=0. \tag{2.25}$$

The term T^4 can also be produced as a linear function of temperature as

$$T^4=T_a^4+4\,T_a^3\,(T-T_a)+6\,T_a^2\,(T-T_a)^2\ldots\approxeq 4\,T_a^3\,T-3\,T_a^4. \tag{2.26}$$

When Eq. (2.26) is substituted into Eq. (2.25), it yields

$$\frac{d^2T}{dx^2}+\frac{16\,\sigma}{3\,k_{eff}\,\beta_R}\left(\frac{d^2T}{dx^2}\right)-\frac{\rho\,c_p\,g\,K\,\beta_R}{t\,v\,k_{eff}}\left(T-T_a\right)^2\,sin(\gamma)$$
$$-\frac{h\,P\,(1-\epsilon)\,(T-T_a)}{t\,k_{eff}}-\frac{4\,T_a^3\,\sigma\,\epsilon}{t\,k_{eff}}\,(T-T_a)-\frac{\sigma\,B_0^2\,u^2}{k_{eff}\,A_{cr}}\,(T-T_a)=0. \tag{2.27}$$

Applying the following non-dimensional parameters from Eq. (2.28) to Eq. (2.27),

$$X=\frac{x}{L},\ \theta=\frac{T-T_a}{T_b-T_a},\ S_h=\frac{g\,K\,\beta_R\,(T_b-T_\infty)\,L}{\alpha\,v\,k_r},\ N_c=\frac{h\,L}{k_{eff}\,t},\ H=\frac{\sigma\,B_0^2\,u^2\,b}{k_{eff}\,A_b},$$
$$R_d=\frac{4\,\sigma_{st}\,T_a^3}{3\,\beta_R\,k_{eff}},\ Nc=\frac{4\,\sigma_{st}\,L\,T_a^3}{t\,k_{eff}}. \tag{2.28}$$

One acquires the non-dimensional form of the governing Eq. (2.27) as presented in Eq. (2.29),

$$(1+4\,R_d)\,\frac{d^2\theta}{dX^2}-S_h\,sin(\gamma)\,\theta^2-N_c\,(1-\epsilon)\,\theta-H\,\theta=0, \tag{2.29}$$

and the non-dimensional boundary conditions are given as follows:

$$X=0,\ \ \frac{d\theta}{dX}=0,$$
$$X=1,\ \ \theta=1. \tag{2.30}$$

3. Approximate analytical solution using the Ananthaswamy-Sivasankari Method

An effective technique known as the Ananthaswamy-Sivasankari method (ASM) is presented [5, 34, 35] for the purpose of employing non-linear ordinary differential equations. The method described here can be used to resolve both non-linear as well as linear differential equations. This method can also be easily modified to address other non-linear problems, such as boundary value issues that occur in the chemical, physical, and applied sciences, particularly fin issues. Moreover, the boundary and initial value problems can be solved using the new approach that has been suggested. For the differential equation and its derivatives, additional boundary conditions can be generated.

The essential concept of ASM is described in Appendix A. We have assumed the solution, which has exponential form and unknown parameters, according to the approach utilized. In order to determine the value of the unknown parameter that appears in the solution, we have used the given boundary condition.

3.1. **Approximate analytical solution for Model-1.** The approximate analytical solution of the temperature distribution in Eq. (2.10) that satisfies the conditions at the boundary are as follows:

$$\theta(\zeta) = l\, e^{b\,\zeta} + m\, e^{-b\,\zeta}, \tag{3.1}$$

$$\theta'(\zeta) = l\, b\, e^{b\,\zeta} - m\, b\, e^{-b\,\zeta}. \tag{3.2}$$

Utilizing the conditions at the boundary in Eq. (2.11), we obtain the values of the parameters l, m and b as follows:

$$m = \frac{e^{b}}{e^{b} + e^{-b}} \quad and \quad l = \frac{e^{-b}}{e^{b} + e^{-b}}. \tag{3.3}$$

Thus the Eq. (3.1), becomes

$$\theta(\zeta) = \frac{e^{-b}\, e^{b\,\zeta} + e^{b}\, e^{-b\,\zeta}}{e^{b} + e^{-b}}. \tag{3.4}$$

Now, by putting the Eq. (3.4) into Eq. (2.10) and then simplifying, we obtain

$$b^2 \left(\frac{e^{-b}\, e^{b\,\zeta} + e^{b}\, e^{-b\,\zeta}}{e^{b} + e^{-b}} \right) - \frac{R_a}{(1 + 4\, R_d)} \left(\frac{e^{-b}\, e^{b\,\zeta} + e^{b}\, e^{-b\,\zeta}}{e^{b} + e^{-b}} \right)^2 - \frac{[N_c\,(1-\epsilon) + N_r + H]}{(1 + 4\, R_d)} \left(\frac{e^{-b}\, e^{b\,\zeta} + e^{b}\, e^{-b\,\zeta}}{e^{b} + e^{-b}} \right) = 0. \tag{3.5}$$

Now taking $\zeta = 0$, Eq. (3.5) becomes

$$b^2 - \frac{R_a}{(1 + 4\, R_d)} - \frac{[N_c\,(1-\epsilon) + N_r + H]}{(1 + 4\, R_d)} = 0. \tag{3.6}$$

On solving Eq. (3.6), we get the value of the parameter b which is given by

$$b = \pm \sqrt{\frac{R_a + N_c\,(1-\epsilon) + N_r + H}{(1 + 4\, R_d)}}. \tag{3.7}$$

Hence, an approximate analytical solution of the temperature is given by

$$\theta(\zeta) = \frac{e^{-b}\, e^{b\,\zeta} + e^{b}\, e^{-b\,\zeta}}{e^{b} + e^{-b}}, \tag{3.8}$$

where b is obtained in Eq. (3.7).

3.1.1. *Fin Efficiency.* Fin efficiency is another way to describe fin attainment and it can be defined as

$$\eta = \frac{q_f}{q_{max}} = \frac{(1 + 4\, R_d)\, \frac{d\theta}{d\zeta}\big|_{\zeta=0}}{[R_a + N_c\,(1-\epsilon) + N_r + H]}. \tag{3.9}$$

3.2. **Approximate analytical solution for Model-2.** The approximate analytical solution of the temperature distribution in Eq. (2.29) that satisfies the boundary conditions are as follows:

$$\theta(X) = l\, e^{n\,X} + m\, e^{-n\,X}, \tag{3.10}$$

$$\theta'(X) = l\, n\, e^{n\,X} - m\, n\, e^{-n\,X}. \tag{3.11}$$

Utilizing the boundary conditions in Eq. (2.30), we obtain the values of the parameters l, m and n as follows:

$$l = m \quad and \quad l = \frac{1}{e^{n} + e^{-n}}. \tag{3.12}$$

Thus the Eq. (3.10), becomes

$$\theta(X) = \frac{e^{n\,X} + e^{-n\,X}}{e^{n} + e^{-n}}. \tag{3.13}$$

Now, by putting the Eq. (3.13) into Eq. (2.29) and then simplifying, we obtain

$$(1+4\,R_d)\; n^2 \left(\frac{e^{n\,X} + e^{-n\,X}}{e^{n} + e^{-n}}\right) - S_h\, sin(\gamma) \left(\frac{e^{n\,X} + e^{-n\,X}}{e^{n} + e^{-n}}\right)^2 - N_c\,(1-\epsilon) \left(\frac{e^{n\,X} + e^{-n\,X}}{e^{n} + e^{-n}}\right) - H \left(\frac{e^{n\,X} + e^{-n\,X}}{e^{n} + e^{-n}}\right) = 0. \tag{3.14}$$

Now, taking $X = 1$ Eq. (3.14) becomes

$$(1+4\,R_d)\; n^2 - S_h\, sin(\gamma) - N_c\,(1-\epsilon) - H = 0. \tag{3.15}$$

On solving the Eq. (3.15), we get the value of the parameter n, which is given by

$$n = \pm\sqrt{\frac{S_h\, sin(\gamma) + N_c\,(1-\epsilon) + H}{(1+4\,R_d)}}. \tag{3.16}$$

Hence, an approximate analytical solution of the temperature is obtained by substituting Eq. (3.16) into Eq. (3.13) as follows:

$$\theta(X) = \frac{cosh\, n\, X}{cosh\, n}, \tag{3.17}$$

where n is obtained in Eq. (3.16).

3.2.1. *Thermal performance indicator: Rate regarding heat transfer in a porous fin.* The rate for heat transfer from the fin base is given by

$$q_b = k\, A_c\, \frac{dT}{dx}. \tag{3.18}$$

Using the non-dimensional parameters in Eq. (2.17), one arrives at the fin-base dimensionless heat transfer rate as

$$Q_b = \frac{q\, L}{k\, A_c\,(T_b - T_\infty)} = \left[\frac{d\theta}{dX}\right]_{X=1}. \tag{3.19}$$

4. Results and discussion

Here, we have discussed the results obtained by this proposed method in graphical representation for the considered models. For both models, we have derived an approximate analytical solution. By comparing those results with the numerical solution, our results reach a considerable conclusion. The results are compared with the help of MATLAB software. Numerous parameters involved in the problem were displayed without losing their significance.

When buoyancy and Lorentz forces are balanced, the flow is determined by the parameter R_a, which measures the proportion of diffusion to thermal convection. The strength of surface radiation against conduction is measured by parameter N_r, while the intensity of convection against conduction is represented by the parameter N_c. The ratio of electromagnetic force with viscous force is analyzed by the parameter H.

For Model-1: Figures 4 to 9 show a comparison regarding the numerical solution reported in [24] with the analytical solution using Eq. (3.8) of dimensionless temperature $\theta(\zeta)$ with the dimensionless fin length ζ for Eq. (2.10). Figure 4 illustrates that by increasing the value of N_r, the temperature $\theta(\zeta)$ falls. Strong cooling predicts less radiant temperature distribution in the fin, as the results demonstrate when the fin temperature drops with N_r. Figure 5 demonstrates that the temperature $\theta(\zeta)$ drops by raising the amount of N_c. The findings indicate that when N_c increases, the fin temperature drops, leading to a more substantial drop in the local temperature in the insulated tip fin. Figure 6 displays that as the value of Hartmann number H increases, the temperature $\theta(\zeta)$ decreases. Figure 7 reveals that the temperature $\theta(\zeta)$ decreases as the modified Rayleigh number R_a raises. Consequently, when it comes to a rectangular porous fin, the illustration in Figure 7 undoubtedly shows that the radiation-conduction variable exhibits a minimal impact on the fin's surface temperature. Figure 8 indicates that by increasing the radiation-conduction parameter R_d, the temperature $\theta(\zeta)$ increases. Figure 9 shows that the temperature $\theta(\zeta)$ rises by increasing the amount of the porosity parameter ϵ.

Figures 10 to 13 represent the fin efficiency η using Eq. (3.9) of Eq. (2.10). Figure 10 demonstrates the fin efficiency η with the dimensionless modified Rayleigh number R_a. In this figure, by increasing the value of the porosity parameter ϵ, the fin efficiency η drops. Figure 11 illustrates the fin efficiency η with the dimensionless radiation-conduction parameter R_d. According to this figure, the fin efficiency η drops by increasing the value of the porosity parameter ϵ. Figure 12 shows the fin efficiency η with the dimensionless surface ambient parameter N_r. This graph shows that raising the porosity parameter ϵ value causes a decrease in fin efficiency. Figure 13 demonstrates the fin efficiency η through the dimensionless convection-conduction parameter N_c. Based on this figure, the fin efficiency diminishes as the value of the porosity parameter ϵ increases. Table 1 displays several dimensionless temperature $\theta(\zeta)$ values that were obtained by ASM, ADSTM, LSM, and NM for particular amounts of the parameters N_r, N_c, H, R_a, R_d, ϵ. This table shows that the average absolute error percentage was 0.5. In comparison to our analytical method, selecting a polynomial in ADSTM was quite tedious and evaluating values in LSM & NM take a lot of time. The comparison reveals a strong agreement, as seen in Table 1 and Figures 4-9. For this reason, we are assured with the accuracy of the current results.

For Model-2: Figures 14 to 19 depict a comparison of the numerical solution reported in [29] with the analytical solution using Eq. (3.17) of dimensionless temperature $\theta(X)$ with the dimensionless fin length X for Eq. (2.29). Figure 14 shows that by increasing the value of γ, the temperature $\theta(X)$ increases. The reason for the decrease in the fin's local temperature with increasing fin inclination is the increased force that drives for buoyancy and convection of the fluid in action surrounding the expanded surface. Figure 15 demonstrates that the temperature $\theta(X)$ drops by raising the amount of H. A drop in the temperature of the fin is the result of a boost in the Lorentz force, which is caused by a rise in the magnetic parameter or Hartmann number. This resistive force prevents the fluid that works surrounding the fin from moving. Figure 16 displays that as the dimensionless convection number N_c increases, the temperature $\theta(X)$ decreases. This occurs because a higher level of heat is removed on the fin surface when convective and radiative parameters rise, which subsequently raises the impacts of convective and radiative heat transfer upon the fin surface. Consequently, when the convective and radiative factors go up, the fin's surface temperature falls (i.e. the fin temperature profile decreases) and its heat transfer rate grows. Relatively thick and short fins with extreme thermal conductivity are implied by small amounts of the convective as well as radiative parameters, N_c and R_a, whereas relatively thin and extended fins with minimal thermal conductivity are suggested by a large value of the related parameters. Thus, minimal amounts of convective and radiative parameters promote the fin's thermal efficiency, meaning that a relatively thick, short fin with a high thermal conductivity is preferred. Figure 17 depicts that the temperature $\theta(X)$ decreases as the dimensionless porosity parameter S_h rises. The fin temperature decreases as the porosity parameter increases because of the increase in the permeability of the fin, which makes the working fluid infiltrate more through the pores of the fin and increases the buoyancy force effect. Consequently, more heat is taken away from the surface of the fin as the temperature falls more. This establishes that the thermal efficiency of the fin increases as the Rayleigh number is enlarged. Figure 18 shows that by increasing the radiation-conduction parameter R_d, the temperature $\theta(X)$ increases. Figure 19 indicates that the temperature $\theta(X)$ rises by increasing the amount of porosity or void ratio ϵ.

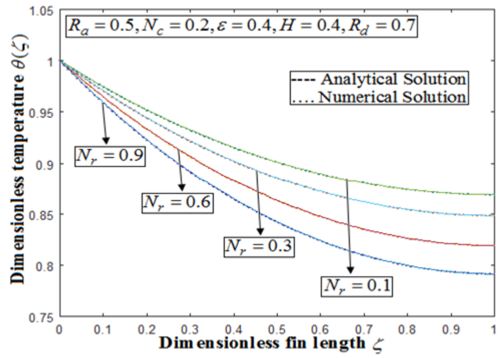

FIGURE 4. Variation of dimensionless surface ambient parameter on the temperature profile.

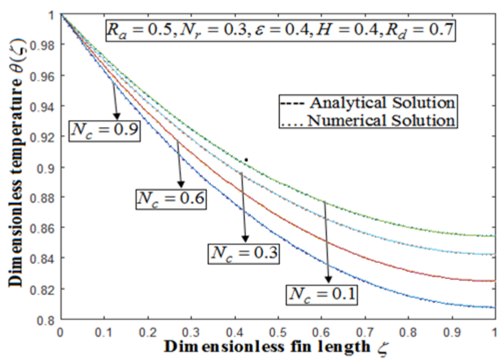

FIGURE 5. Effects of dimensionless convection-conduction parameter on the temperature profile.

Figures 20 to 23 represent the rate related to heat transfer using Eq. (3.19) of Eq. (2.29). Figure 20 depicts the rate related to heat transfer Q_b with the dimensionless radiation number R_d. According to this figure, by increasing the value of the Hartmann number H, the rate of heat transfer Q_b increases. Figure 21 shows the rate related to heat transfer Q_b with the dimensionless convection number N_c. Based on this figure, the rate related to heat transfer rises by increasing the value of the porosity parameter S_h. Figure 22 displays the rate related to heat transfer with the dimensionless porosity parameter S_h. This graph shows that raising the porosity or void ratio ϵ value causes a decrease in heat transfer rate. Figure 23 demonstrates the rate related to heat transfer Q_b with the dimensionless porosity or void ratio ϵ. From this figure, the rate related to heat transfer increases as the value of the convection number N_c rises. Table 2 examines the analytical and numerical results of dimensionless temperature $\theta(X)$ for some particular values of the parameters. According to this table, the average absolute error percentage was 0.2.

The main contribution of our work is pointed out below:

- Analytical approximations were derived using the presented technique.
- For both models, the solution was given in explicit form and the results were plotted.
- The fin efficiency and heat transfer rate were calculated and displayed graphically.
- Furthermore, at smaller amounts of the fin inclination, convective, porous, magnetic, and radiative characteristics, the porous fin with inclination is highly effective as well as efficient. To prevent thermal stability within the fin, these parameters should be carefully chosen.
- In thermal and electronic systems, the current findings will assist in designing passive heat enhancement and choosing the appropriate fin material.
- We have concluded from the two models that the technique used is significantly more precise than alternative analytical and numerical approaches.

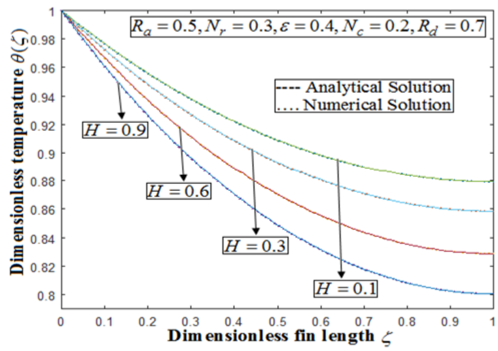

FIGURE 6. Variation of the Hartmann parameter in the temperature profile.

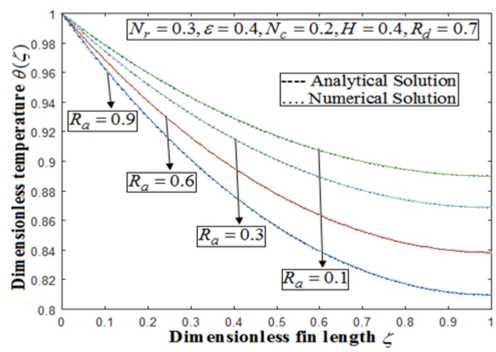

FIGURE 7. Impacts of dimensionless modified Rayleigh number on the temperature profile.

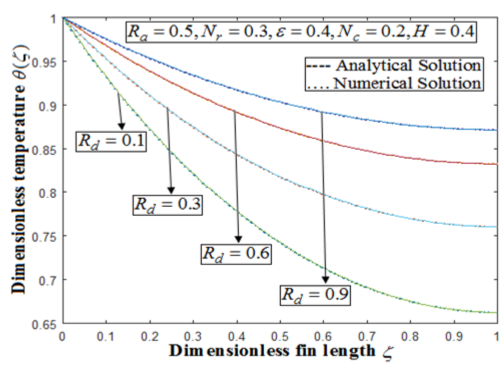

FIGURE 8. Variation of dimensionless radiation-conduction parameter in the temperature profile.

CONCLUSION

Two different models of rectangular porous fins were analytically studied using a new approximate analytical method, ASM, and the findings were compared with the numerical method, which resulted in a very good agreement. The influence of different physical parameters taking part in the problem was illustrated graphically. The fin efficiency and the rate related to heat transfer were also calculated and displayed. Furthermore, it has been discovered that this technique is a strong mathematical tool that may be used to solve a wide range of linear as well as non-linear issues that arise in various branches of science and engineering.This technique will be extended in the future to handle non-linear

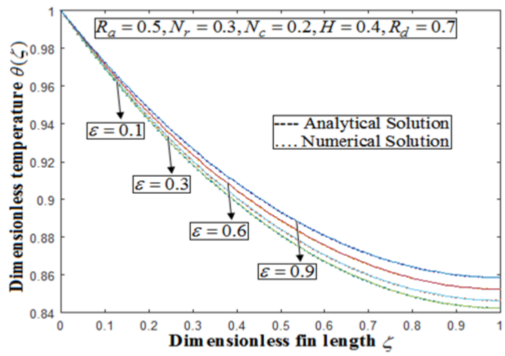

FIGURE 9. Effects of dimensionless porosity parameter on the temperature profile.

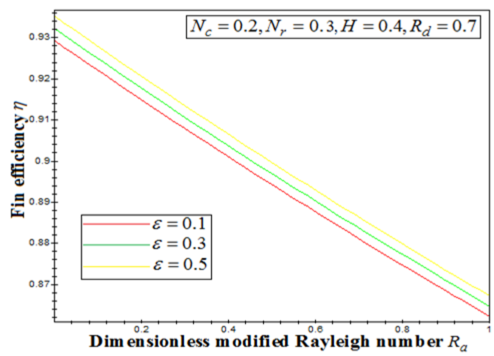

FIGURE 10. Effects of ϵ on fin efficiency with dimensionless modified Rayleigh number.

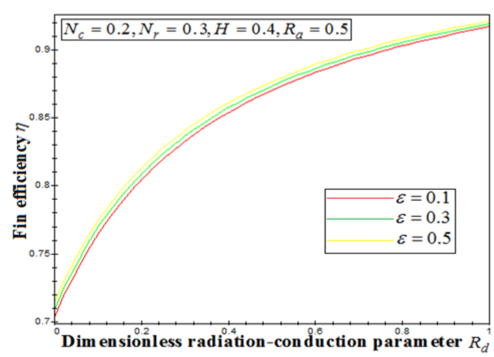

FIGURE 11. Effects of ϵ on fin efficiency with dimensionless radiation-conduction parameter.

PDEs and infinite boundary value problems. In the future, we can employ this method to solve the mathematical models of non-linear partial differential equations in both dimensional and dimensionless form.
The following points are concluded from the results:
• For both models,the temperature drops as the values of the Hartmann number, radiation parameter, and convection parameter rise.
• Both models experience a rise in temperature with increasing porosity, or void ratio and radiation number.
• The fin efficiency for model-1 increases with increasing porosity parameter values.

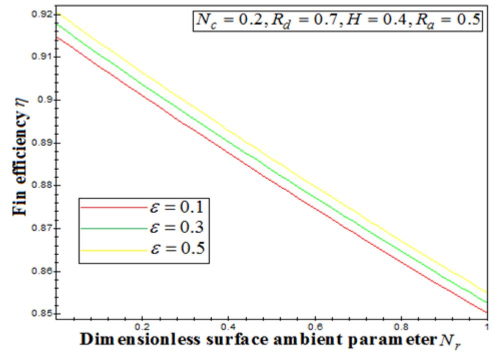

FIGURE 12. Effects of ϵ on fin efficiency with dimensionless surface ambient parameter.

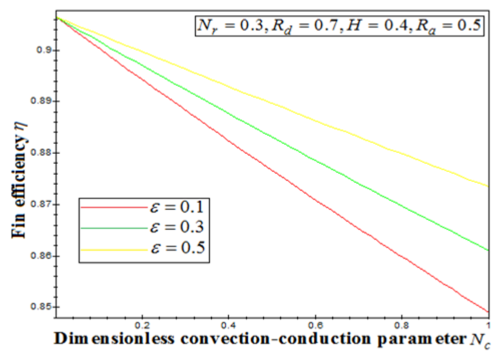

FIGURE 13. Effects of ϵ on fin efficiency with dimensionless convection-conduction parameter.

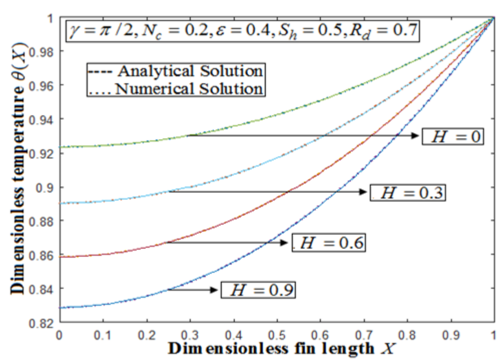

FIGURE 14. Variation of angle of inclination on the temperature profile.

• For model-2, increasing the porosity, convection, and Hartmann numbers enhances the rate related to heat transfer, whereas increasing the void ratio decreases the rate related to heat transfer.
• The thermal performance of the fin is significantly influenced by the angle of inclination for model-2.

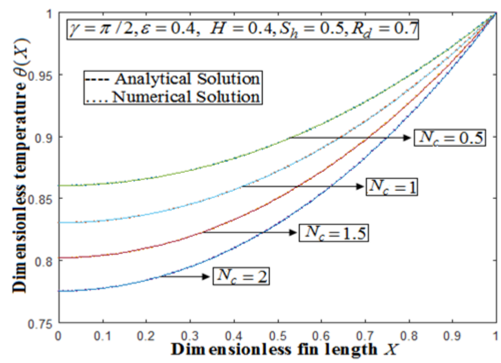

FIGURE 15. Impacts of dimensionless Hartmann number in the temperature profile.

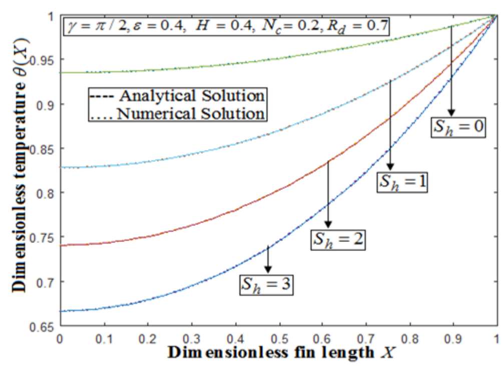

FIGURE 16. Variation of dimensionless convection number on the temperature profile.

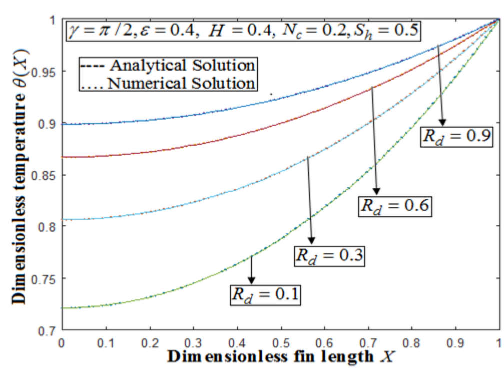

FIGURE 17. Effects of dimensionless porosity parameter in the temperature profile.

APPENDIX

Appendix A: Basic Concept of the Ananthaswamy-Sivasankari Method [4, 6, 28]. Let us consider the non-linear boundary value problem:

$$p : g(z, z', z'') = 0, \tag{A. 1}$$

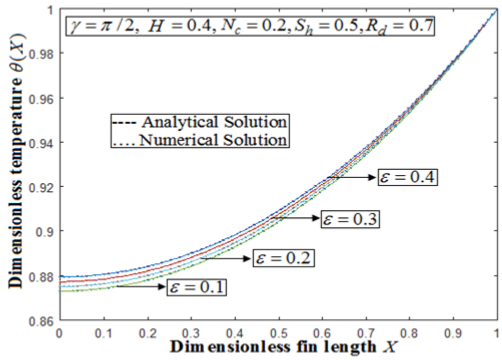

FIGURE 18. Impacts of dimensionless radiation number on the temperature profile.

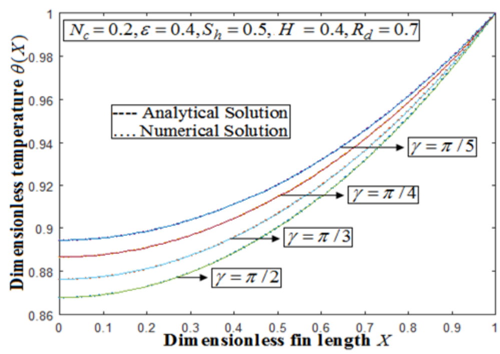

FIGURE 19. Variation of porosity or void ratio on the temperature profile.

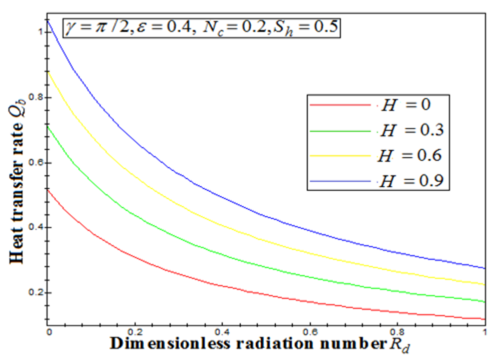

FIGURE 20. Effects of Hartmann number H on heat transfer rate Q_b with dimensionless radiation number.

where p indicates the second-order non-linear differential equation such that $z = z(x, r, s, ...)$ in which r, s are given parameters and $x \in [L, U]$ can be finite or infinite considering the associated conditions at the boundary:

$$\begin{cases} At \quad x = L, \;\; z(x) = z_{L_0} \;\; (or) \;\; z'(x) = z_{L_1}, \\ At \quad x = U, \;\; z(x) = z_{U_0} \;\; (or) \;\; z'(x) = z_{U_1}. \end{cases} \tag{A. 2}$$

Assume that the approximate analytical solution for the non-linear equations is an exponential function of the form

$$z(x) = ke^{hx} + le^{-hx}. \tag{A. 3}$$

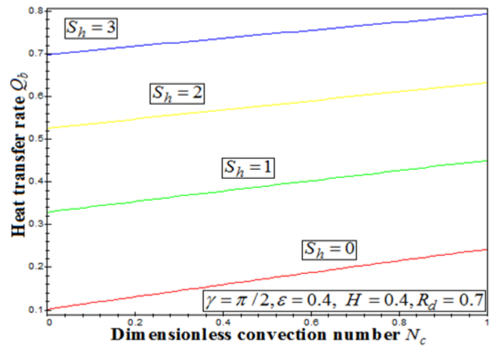

FIGURE 21. Effects of dimensionless porosity parameter S_h on heat transfer rate Q_b with dimensionless convection number.

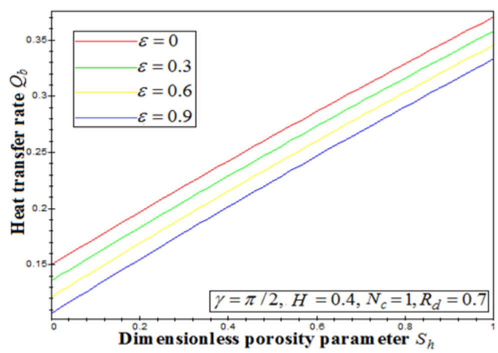

FIGURE 22. Effects of porosity or void ratio ϵ on heat transfer rate Q_b with dimensionless porosity parameter.

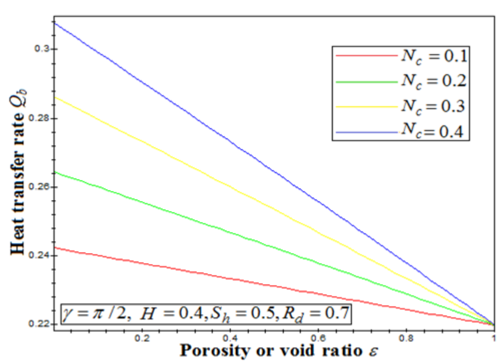

FIGURE 23. Effects of dimensionless convection number N_c on heat transfer rate Q_b with porosity parameter.

By resolving the following non-linear differential equations, the unknown coefficients k and l are discovered:

$$\begin{cases} z(L) = ke^{hL} + le^{-hL} & = z_{L_0}, \\ z'(L) = hke^{hL} - hle^{-hL} & = z_{L_1}, \end{cases} \tag{A. 4}$$

$$\begin{cases} z(U) = ke^{hU} + le^{-hU} & = z_{U_0}, \\ z'(U) = hke^{hU} - hle^{-hU} & = z_{U_1}. \end{cases} \tag{A. 5}$$

Table 1. Comparison of numerical and analytical solutions of Eq. (2.10) for some fixed values of the parameters $N_r = 0.3$, $N_c = 0.2$, $\epsilon = 0.4$, $H = 0.9$, $R_a = 0.1$ and $R_d = 0.5$ for model-1.

ζ	**Dimensionless temperature $\theta(X)$**				
	ASM (3.8)	**ADSTM** [32]	**LSM** [17]	**NM** [32]	**Error b/w ASM & NM**
0	1.000000000	1.000000000	1.000000000	1.000000000	0.000000000
0.1	0.958487073	0.956987943	0.956987665	0.956988020	0.15639783
0.2	0.921896486	0.919132442	0.919132060	0.919132513	0.29986295
0.3	0.890040325	0.886217887	0.886217828	0.886217964	0.42945931
0.4	0.862754992	0.858057590	0.858057970	0.858057690	0.5449925
0.5	0.839900364	0.834492402	0.834492969	0.834492509	0.64386863
0.6	0.821359068	0.815389550	0.815389906	0.815389668	0.72677106
0.7	0.807035887	0.800641676	0.800641589	0.800641805	0.79229215
0.8	0.796857262	0.790166063	0.790165668	0.790166187	0.83968300
0.9	0.790770921	0.783904049	0.783903760	0.783904154	0.8683636
1	0.788745608	0.781820594	0.781820569	0.781820729	0.8779610
Average Absolute Error Percentage					0.5617865

Table 2. Comparison of both analytical and numerical solutions of Eq. (2.29) for some specified values of the parameters $\gamma = \frac{\pi}{2}$, $N_c = 0.2$, $\epsilon = 0.4$, $S_h = 0.5$, $H = 0.4$ and $R_d = 0.7$ for model-2.

X	**Dimensionless temperature $\theta(X)$**		
	Analytical Solution (3.17)	**Numerical Solution** [36]	**Error**
0	0.8636040456	0.863499105	0.012151
0.2	0.8689274874	0.868776234	0.017407
0.4	0.8849634435	0.884696487	0.030166
0.6	0.9119096113	0.911530621	0.04156
0.8	0.9500981947	0.949741193	0.037575
1	1	1	0
Average Error Percentage			0.023143

The unknown parameters k and l may be calculated via Eqs. (A. 4) and (A. 5).

The following non-linear differential equations are formed by putting Eq. (A. 3) into Eq. (A. 1).

$$p : g(z(x,k,l,h,r,s), z'(x,k,l,h,r,s), z''(x,k,l,h,r,s)) = 0. \tag{A. 6}$$

This equation holds true at x, where $x \in [L, U]$. By tackling Eq. (A. 6), the unknown value of the parameter h can be discovered in terms of the existing parameters r and s.

Symbol	Meaning
A	Cross sectional area
L	Fin length
W	Width
A_b	Porous fin base area
c_p	Specific heat capacity of the fluid passing through porous fin
t	Fin thickness
h	Heat transfer coefficient
u	Fluid average velocity
v	Kinematic viscosity
w	Width of the fin
x	Axial length of the fin
k_{eff}	Effective thermal conductivity
J_C	Conduction current intensity
J	Total current intensity
$\bar{m}$	The mass flow rate of the fluid
$\bar{v_w}$	Passage velocity
T_b	Temperature at the fin base
T	Fin temperature
T_a	Ambient temperature
γ	Angle of inclination
ϵ	Porosity or void ratio
X	Dimensionless fin length
θ	Dimensionless temperature
ζ	Dimensionless fin length
S_h	Dimensionless porosity parameter
Q_b	Heat transfer rate
R_a	Modified Rayleigh number
R_d	Radiation–conduction parameter
N_r	Surface ambient parameter
N_c	Convection-conduction parameter
H	Hartmann parameter
NM	Numerical Method
LSM	Least Square Method
ADSTM	Adomian Decomposition Sumudu Transform Method
PM	Perturbation Method

Appendix C: Nomenclature.

Conflict of interests

The authors declare that there is no conflict of interests.

Acknowledgement

The authors are very grateful to the reviewers for carefully reading the paper and for their comments and suggestions which have improved the paper.

References

[1] M. Alkam and M. Al-Nimr,*Improving the performance of double-pipe heat exchangers by using porous substrates*, Int. J. Heat Mass Transfer,*42* (1999), 3609–3618.

[2] S. R. Amirkolaei, D. D. Ganji, and H. Salarian, *Determination of temperature distribution for porous fin which is exposed to Uniform Magnetic Field to a vertical isothermal surface by Homotopy Analysis Method and Collocation Method*, Indian J. Sci. Res., *1*(2) (2014), 215–222.

[3] A. Aziz and M. N. Bouaziz, *A least squares method for a longitudinal fin with temperature dependent internal heat generation and thermal conductivity*, Energy Convers. Manage., *52* (2011), 2876–2882.

[4] Balaram Kundu and Dipankar Bhanja, *An analytical prediction for performance and optimum design analysis of porous fins*, International Journal of Refrigeration, *34* (2011), 337–352.

[5] J. Chitra,V. Ananthaswamy, S. Sivasankari, and Seenith Sivasaundaram, *A new approximate analytical method (ASM) for solving non-linear boundary value problem in heat transfer through porous fin*, Mathematics in Engineering, Science and Aerospace (MESA) (ISSN: 2041-3065), *14*(1) (2023), 53–69.

[6] R. Das and K. Dilip Prasad, *Prediction of porosity and thermal diffusivity in a porous fin using differential evolution algorithm*, Swarm and Evolutionary Computation, *23* (2015), 27–39.

[7] R. Das and K. T. Ooi, *Predicting multiple combination of parameters for designing a porous fin subjected to a given temperature requirement*, Energy Conversion and Management, *66* (2013), 211–219.

[8] Dipankar Bhanja, Balaram Kundu, and Pabitra Kumar Mandal, *Thermal analysis of porous pin fin used for electronic cooling*, Procedia Engineering, *64* (2013), 956–965.

[9] D. D. Ganji, Y. Rostamiyan, I. Rahimi Petroudi, and M. Khazayi Nejad, *Analytical investigation of nonlinear model arising in heat transfer through the porous fin*, Thermal sciences, *18* (2014), 409–417.

[10] S. E. Ghasemi, P. Valipour, M. Hatami, and D. D. Ganji, *Heat transfer study on solid and porous convective fins with temperature-dependent heat generation using efficient analytical method*, Journal of Central South University, *21*(12) (2014), 4592–4598.

[11] S. E. Ghasemi, M. Hatami, and D. D. Ganji, *Thermal analysis of convective fin with temperature-dependent thermal conductivity and heat generation*, Case Studies in Thermal Engineering, *4* (2014), 1–8.

[12] B. J. Gireesha and G. Sowmya, *Heat transfer analysis of an inclined porous fin using differential transform method*, International Journal of Ambient Energy, *43*(1) (2020), 3189–3195.

[13] M. Hatami and D. D. Ganji, *Thermal behaviour of longitudinal convective–radiative porous fins with different section shapes and ceramic materials* (SiC *and* Si_3N_4), Ceramics International, *40*(5) (2015), 6765–6775.

[14] M. Hatami, G. R. M. Ahangar, D. D. Ganji, and K. Boubaker, *Refrigeration efficiency analysis for fully wet semi-spherical porous fins*, Energy Conversion and Management, *84* (2014), 533–540.

[15] M. Hatami and D. D. Ganji, *Thermal and flow analysis of microchannel heat sink (MCHS) cooled by Cu–water nanofluid using porous media approach and least square method*, Energy Conversion and Management, *78* (2014), 347–358.

[16] M. Hatami, A. Hasanpour, and D. D. Ganji, *Heat transfer study through porous fins (*Si_3N_4 *and Al) with temperature-dependent heat generation*, Energy Conversion and Management, *74* (2013), 9–16.

[17] H. A. Hoshyar, D. D. Ganji, and A. R. Majidian, *Least square method for porous fin in the presence of uniform magnetic field*, Journal of Applied Fluid Mechanics, *9* (2016), 661–668.

[18] H. H. Jasim and M. S. Söylemez, *Optimization of a rectangular pin fin using rectangular perforations with different inclination angles*, International Journal of Heat and Technology, *35*(4) (2017), 969–977.

[19] F. Khani, M. Ahmadzadeh Rajib, and H. Hamedi Nejad, *Analytical solutions and efficiency of the nonlinear fin problem with temperature-dependent thermal conductivity and heat transfer coefficient*, Communications in Nonlinear Science and Numerical Simulation, *14*(8) (2009), 3327–3338.

[20] S. Kiwan and M. Al-Nimr, *Enhancement of heat transfer using porous fins*, ASME J. Heat Transfer, *123*(4) (2001), 790–795.

[21] S. Kiwan and O. Zeitoun, *Natural convection in a horizontal cylindrical annulus using porous fins*, Int. J. Numer. Methods Heat Fluid Flow, *18*(5) (2008), 618–634.

[22] S. Kiwan, *Effect of radiative losses on the heat transfer from porous fins*, Int. J. Therm. Sci., *46* (2007), 1046–1055.

[23] Kuljeet Singh, Ranjan Das, and Balaram Kundu, *Approximate analytical method for porous stepped fins with temperature-dependent heat transfer parameters*, Journal of Thermo physics and Heat Transfer, *30* (2016), 661–672.

[24] R. Li, J. Manafian, H. A. Lafta, H. A. Kareem, K. F. Uktamov, and M. Abotaleb, *The nonlinear vibration and dispersive wave systems with cross-kink and solitary wave solutions*, International Journal of Geometric Methods in Modern Physics, *19*(10) (2022).

[25] R. Li, Z. A. B. Sinnah, Z. M. Shatouri, J. Manafian, M. F. Aghdaei, and A. Kadi, *Different forms of optical soliton solutions to the Kudryashov's quintuple self-phase modulation with dual-form of generalized nonlocal nonlinearity*, Results in Physics, *46* (2023).

[26] S. Mosayebidorcheh, M. Farzinpoor, and D. D. Ganji, *Transient thermal analysis of longitudinal fins with internal heat generation considering temperature-dependent properties and different fin profiles*, Energy Conversion and Management, *86* (2014), 365–370,

[27] G. A. Oguntala, M. G. Sobamowo, A. A. Yinusa, and R. Abd-Alhameed, *Application of approximate analytical technique using the Homotopy perturbation method to study the inclination effect on the thermal behaviour of porous fin heat sink*, Mathematical and Computational Applications, *23* (2018), 62,

[28] G. A. Oguntala, M. G. Sobamowo, R. Abd-Alhameed, and J. Noras, *Numerical investigation of inclination on the thermal performance of porous fin heat sink using Pseudo-spectral collocation method*, Karbala International Journal of Modern Science, *5*(1) (2009), 19–26.

[29] G. A. Oguntala, R. A. Abd-Alhameed, M. G. Sobamowo, and I. Danjuma, *Performance, thermal stability and optimum design analyses of rectangular fin with temperature-dependent thermal properties and internal heat generation*, Journal of Computational Applied Mechanics, *49* (2018), 37–43,

[30] G. A. Oguntala, R. A. Abd-Alhameed, M. G. Sobamowo, and N. Eya, *Effects of particles deposition on thermal performance of a convective-radiative heat sink porous fin of an electronic component*, Thermal Science and Engineering Progress, *6* (2018), 177–185.

[31] G. A. Oguntala, R. A. Abd-Alhameed, and M. G. Sobamowo, *On the effect of magnetic field on thermal performance of convective-radiative fin with temperature-dependent thermal conductivity*, Karbala International Journal of Modern Science, *4* (2018), 1–11.

[32] T. Patel and R. Meher, *Thermal analysis of porous fin with uniform magnetic field using Adomian decomposition Sumudu transform method*, Nonlinear Engineering, *6*(3) (2017), 191–200.

[33] R. Siegel and J. R. Howell, *Thermal Radiation Heat Transfer*, 3rd edn, Chap. 12. Hemisphere, Washington, DC (1992).

[34] S. Sivasankari and V. Ananthaswamy, *A mathematical study on non-linear ordinary differential equation for Magnetohydrodynamic flow of the Darcy-Forchheimer nanofluid*, Computational Methods for Differential Equations, *11*(4) (2023), 696–715.

[35] S. Sivasankari, V. Ananthaswamy, and Seenith Sivasundaram, *A new approximate analytical method for solving some non-linear initial value problems in physical sciences*, Mathematics in Engineering, Science and Aerospace (MESA) (ISSN: 2041-3065), *14*(1) (2023), 145-162.

[36] M. G. Sobamowo, *Combined impacts of fin surface inclination and Magnetohydrodynamic on the thermal performance of a convective-radiative porous fin*, Journal of Applied and Computational Mechanics, *8*(3) (2022), 940–948.

[37] M. G. Sobamowo, K. C. Alaribe, O. A. Adeleye, A. A. Yinusa, and O. A. Adedibu, *A study on the impact of Lorentz force on the thermal behaviour of a convective-radiative porous fin using Differential Transformation Method*, International Journal of Mechanical Dynamics and Analysis, *6*(+1) (2020), 45–59.

[38] M. G. Sobamowo, O. M. Kamiyo, and O. A. Adeleye, *Thermal performance analysis of a natural convection porous fin with temperature-dependent thermal conductivity and internal heat generation*, Thermal Science and Engineering Progress, *1* (2017), 39–52.

[39] M. G. Sobamowo, *Thermal analysis of longitudinal fin with temperature-dependent properties and internal heat generation using Galerkin's method of weighted residual*, Applied Thermal Engineering, *99* (2016), 1316–1330.

[40] A. Taklifi, C. Aghanajafi, and H. krami, *The Effect of MHD on a Porous Fin Attached to a Vertical Isothermal Surface*, Transp. Porous Med., *85* (2010), 215–231.